https://doi.org/10.5194/acp-2021-319
Preprint. Discussion started: 21 April 2021

Atmospheric Chemistry and Physics Discussions

High Homogeneous Freezing Onsets of Sulfuric Acid Aerosol at Cirrus Temperatures

Julia Schneider[1], Kristina Höhler[1], Robert Wagner[1], Harald Saathoff[1], Martin Schnaiter[1], Tobias Schorr[1], Isabelle Steinke[2], Stefan Benz[3], Manuel Baumgartner[4,a], Christian Rolf[5], Martina Krämer[5,4], Thomas Leisner[1], and Ottmar Möhler[1]

[1]Institute of Meteorology and Climate Research, Karlsruhe Institute of Technology, Karlsruhe, Germany
[2]Atmospheric Sciences and Global Change Division, Pacific Northwest National Laboratory, Richland, USA
[3]Landesanstalt für Umwelt Baden-Württemberg, Karlsruhe, Germany
[4]Institute for Atmospheric Physics, Johannes Gutenberg University, Mainz, Germany
[5]Institute for Energy and Climate Research, IEK-7: Stratosphere, Research Center Jülich, Jülich, Germany
[a]now at: Deutscher Wetterdienst, Offenbach, Germany

Correspondence: Dr. Ottmar Möhler (ottmar.moehler@kit.edu)

Abstract. Homogeneous freezing of aqueous solution aerosol particles is an important process for cloud ice formation in the upper troposphere. There the air temperature is low, the ice supersaturation can be high, and the concentration of ice-nucleating particles is too low to initiate and dominate cirrus cloud formation by heterogeneous ice nucleation processes. The most common description to quantify homogeneous freezing processes is based on the water activity criterion (WAC) as proposed by Koop et al. (2000). The WAC describes the homogeneous nucleation rate coefficients only as a function of the water activity, temperature and size of the aqueous aerosol particles, which makes this approach well applicable in numerical models. In this study, we investigate the homogeneous freezing behaviour of aqueous sulfuric acid aerosol particles by means of a comprehensive collection of laboratory homogeneous freezing experiments conducted at the AIDA (Aerosol Interaction and Dynamics in the Atmosphere) cloud simulation chamber, which were conducted as part of 17 measurement campaigns since 2007. The most recent experiments were conducted during October 2020 with special emphasis on temperatures below 200 K. Aqueous sulfuric acid aerosol particles were generated at high purity by particle nucleation in a gas flow composed of clean synthetic air and sulfuric acid vapor, which was added to the AIDA chamber. The resulting chamber aerosol had number concentrations from 30 cm^{-3} up to several 1000 cm^{-3} with particle diameters ranging from about 30 nm to 1.1 $\mu\mathrm{m}$. Homogeneous freezing of the aerosol particles was measured at simulated cirrus formation conditions in a wide range of temperatures between 185 K and 230 K with a steady increase of relative humidity during each experiment. At temperatures between about 205 K and about 230 K, the AIDA results agree well with the WAC-based predictions of homogeneous freezing onsets. At lower temperatures, however, the AIDA results show an increasing deviation from the WAC-based predictions towards higher freezing onsets. For temperatures between 185 K and 205 K, the WAC-based ice saturation ratios for homogeneous freezing onsets increase from about 1.6 to 1.7, whereas the AIDA measurements show an increase from about 1.7 to 2.0 in the same temperature range. Based on our experimental results, we suggest a new fit line as a parameterization for the onset conditions of homogeneous freezing of sulfuric acid aerosol particles. As a next step, we propose the new parameterization to be implemented in atmospheric

https://doi.org/10.5194/acp-2021-319
Preprint. Discussion started: 21 April 2021


Atmospheric Chemistry and Physics Discussions

models as an improved version of the WAC-based parameterization from Koop et al. (2000). The new homogeneous freezing thresholds may have significant impacts on the prediction of cirrus cloud occurrence and related cloud radiative effects.

1 Introduction

For predicting the weather and climate on our planet, it is of particular importance to understand and describe the cloud processes in the atmosphere. The evolution of mixed-phase and cirrus clouds is strongly influenced by the presence of cloud ice (Lynch, 2002). Cirrus clouds generally form in the cold upper troposphere and occur in particular in tropical regions but also in mid and high latitudes. By being able to scatter and absorb light, cirrus clouds are an important factor in the global radiation budget. Solid aerosol particles often act as promoter of cloud ice formation in the atmosphere via heterogeneous nucleation at low ice supersaturations. In regions with low concentrations of solid ice-nucleating particles, the homogeneous nucleation of aqueous solution aerosol particles becomes more relevant for cirrus clouds at conditions of lower temperatures and higher ice supersaturations. (Cziczo and Froyd, 2014; Cziczo et al., 2013; Lynch, 2002).

Koop et al. (2000) suggested the water activity criterion (WAC) to predict isolines for the homogeneous freezing rate coefficients of aqueous solutions. This approach (hereafter called Koop2000) was deduced from measurements of the homogeneous freezing temperature observed for different aqueous solutions in dependence on their composition. According to their observations, the ice nucleation behavior only depends on the water activity of the solute, which in thermodynamic equilibrium equals the relative humidity of the surrounding environment (Koop, 2015). Thus, the parameterization of the homogeneous nucleation rate coefficients and related freezing onsets does not depend on the type of the solute, which makes this approach very suitable for atmospheric models.

As aqueous sulfuric acid solution (H_2SO_4/H_2O) aerosol particles are frequently present in the upper troposphere and lower stratosphere, these particles are of particular importance for freezing processes at these altitudes. Therefore, the experiments in this study focus on this aerosol type. Homogeneous freezing onsets of sulfuric acid available from literature are compiled in Table 1 and plotted in Fig. 1 in the water activity-temperature-space. In cases where water activities or relative humidities were not given by the authors, we used the Extended AIM Aerosol Thermodynamics Model (E-AIM) on http://www.aim.env.uea.ac.uk/aim/aim.php (Carslaw et al., 1995; Clegg and Brimblecombe, 1995; Wexler and Clegg, 2002) to transfer given H_2SO_4 concentrations into water activities, which we assume to be equal to relative humidity. For calculating the melting point curve (solid line in Fig. 1), which is the saturation pressure over liquid water in equilibrium with the ice phase, the parameterizations for the saturation pressure over liquid water and ice suggested by Murphy and Koop (2005) have been used. Also shown are homogeneous freezing onset lines calculated according to Koop2000 for nucleation rate coefficients of $J_V = 10^{13}$ cm^{-3}s^{-1} (Δa_w = 0.3, dashed line) and $J_V = 5 \cdot 10^8$ cm^{-3}s^{-1} (Δa_w = 0.32, dotted line) (Möhler et al., 2003).

https://doi.org/10.5194/acp-2021-319
Preprint. Discussion started: 21 April 2021


Atmospheric Chemistry and Physics Discussions

The earliest freezing experiments with aqueous sulfuric acid solutions at variable solute concentrations and temperatures were performed with macroscopic samples (Ohtake, 1993; Beyer et al., 1994; Song, 1994). The observed onsets deviate significantly from Koop2000 with low water activities close to the melting point curve. More recent flow tube experiments, where Fourier transform infrared (FTIR) spectroscopy was used to derive the concentration of freezing sulfuric acid aerosol (Bertram et al., 1996; Clapp et al., 1997), reported lower water activities especially for the freezing onsets at low temperatures ($T <$ 220 K). However, the majority of the compiled freezing onsets in Fig. 1 agree with the Koop2000 predictions considering their measurement uncertainties. Homogeneous freezing experiments performed in the AIDA (Aerosol Interaction and Dynamics in the Atmosphere) cloud simulation chamber (Möhler et al., 2003; Mangold et al., 2005) show a tendency of freezing onsets towards higher water activities compared to Koop2000 at low temperatures ($T <$ 200 K). For T < 200 K, Koop2000 predicts homogeneous freezing thresholds ranging between ice saturation ratios of 1.6 and 1.7. However, atmospheric observations revealed enhanced ice saturation ratios up to 2.0 and higher in this temperature range (Jensen et al., 2005; Lawson et al., 2008; Krämer et al., 2009; Krämer et al., 2020) seemingly contradicting Koop2000 if the assumption holds that ice saturation ratios are unlikely to exceed the homogeneous freezing thresholds in the atmosphere. To explain this discrepancy, the formation of metastable ice phases with higher saturation pressure than stable forms of ice was suggested by various authors (Malkin et al., 2012; Russo et al., 2014). Also, the presence of organic films on the aerosol particles has been discussed, which would slow down the water vapor uptake and thus the aerosol equilibration to the surrounding conditions (Jensen et al., 2005). It was also suggested that parameterizations for the saturation pressure over supercooled liquid water at low temperatures are at least 20% too low (Jensen et al., 2005). Other authors argued that ice nucleation in solutions is accompanied and influenced by the expulsion of ions from the ice lattice (Bogdan and Molina, 2010; Shafique et al., 2016), which form a highly concentrated residual solution. It was suggested that the formation of such mixed-phase cloud particles could produce higher ice supersaturations than expected according to Koop2000 (Bogdan and Molina, 2010).

There are only few in situ measurements of cirrus and their microphysical properties in the field, e.g. in aircraft campaigns (Krämer et al., 2020). These measurements are often limited, as the collection of cloud samples in the atmosphere usually takes place after the onset of ice formation, so that the specific conditions at freezing onset are rarely matched in aircraft studies. However, an improved understanding of atmospheric homogeneous freezing processes can be obtained from laboratory experiments under well controlled conditions. Prompted by the observed tendency of homogeneous freezing onsets towards higher ice saturation ratios than predicted by Koop2000 in previous AIDA studies at low temperatures (Möhler et al., 2003; Mangold et al., 2005), an extended set of homogeneous freezing AIDA experiments focused on the freezing of H_2SO_4/H_2O aerosol particles conducted since 2007 was re-analysed in this study. To quantify the observed trend and the potential deviation to Koop2000 especially at low temperatures, the re-analysed experiments have been complemented by a more recent series of AIDA measurements focusing on temperatures below about 200 K. With this extensive data set of H_2SO_4/H_2O freezing onsets we can provide valuable addition to existing data sets and contribute to a better understanding of homogeneous freezing processes in the atmosphere.

https://doi.org/10.5194/acp-2021-319
Preprint. Discussion started: 21 April 2021


Atmospheric Chemistry and Physics Discussions

2 Methods

2.1 Experimental setup

All experiments have been performed according to experimental procedures as described by Möhler et al. (2003), Benz et al. (2005) and Wagner et al. (2008). Therefore, we only provide a brief summary of the experimental setup and procedures here.

The AIDA facility basically consists of a cloud chamber with 84 m^3 volume, which is situated in a thermal housing and can be cooled to temperatures as low as 183 K. Before starting an experiment, the AIDA cloud chamber is carefully cleaned by evacuating it to a pressure below about 0.1 hPa followed by flushing with dry and particle-free synthetic air several times between 10 hPa and 1 hPa. Then, pure water vapor from a heated liquid water reservoir is added to renew the ice layer on the inner chamber walls and the AIDA is filled with dry synthetic air to ambient pressure. In the cleaned and re-filled chamber, the background aerosol particle concentration is usually lower than 0.1 cm^{-3}.

Fresh sulfuric acid aerosol particles were generated by passing synthetic air over a small amount of concentrated sulfuric acid located in a heated glass tube. Passive cooling of the mixture in the inlet tube was sufficient to induce the homogeneous nucleation of pure H_2SO_4/H_2O particles. The number concentration and size of the particles was controlled by the setting of the tube temperature and the air flow (Wagner et al., 2008). For experiments since 2017, an additional dilution flow of synthetic air was added downstream of the heated glass tube in order to better control the number concentration of generated particles. For example, a reservoir temperature of about 383 K, an air flow of about 0.75 standard $\mathrm{l\,min}^{-1}$ and a dilution flow of about 14 standard $\mathrm{l\,min}^{-1}$ resulted in a median diameter of about 350 nm for the aerosol particles added to the cloud chamber.

A homogeneous distribution of aerosol particles throughout the cloud chamber is achieved by a mixing fan located one meter above the bottom of the chamber. A few minutes after the end of injection, the aerosol particle number concentration and size distribution were measured with a Condensation Particle Counter (CPC 3010, TSI GmbH), an Aerodynamic Particle Sizer (APS 3321, TSI Inc.), and a Scanning Mobility Particle Sizer (SMPS 3934, TSI Inc.), see Sect. 2.2 for details. A cloud expansion experiment is then started by opening the valves to a vacuum pump operated at controlled pump speed. Immediately after pump start, the pressure and thus the temperature inside the chamber start to drop. At the beginning of the experiment, the gas temperature drop is close to adiabatic. However, the increasing temperature difference between the well-mixed chamber interior and the chamber walls, which stay at almost constant temperature, causes an increasing heat flux from the walls to the chamber volume and thereby causes a deviation from the adiabatic temperature profile towards higher gas temperatures. The gas temperature was measured by five vertically and five horizontally aligned temperature sensors. These sensors are calibrated to an accuracy of 0.1 K by direct comparison to a certified platinum resistance temperature sensor (Lake Shore Cryotronics Inc., sensor type PT-103-14L with calibration certificate). The sensor calibration runs are conducted in a chiller bath at temperatures between 293 K and 197 K. We account for an additional uncertainty due to the temperature variability throughout the chamber. The analysis of measurement uncertainties is presented in more detail in Sect. 2.4.

A range of instruments was available for the measurement of gas phase and total water (Wagner et al., 2009). The water vapor pressure was measured inside AIDA by Tunable Diode Laser (TDL) absorption spectroscopy with a time resolution of 1 s using a laser wavelength in the near-infrared of 1370 nm (Fahey et al., 2014). The measurement is done by direct long path

https://doi.org/10.5194/acp-2021-319
Preprint. Discussion started: 21 April 2021


Atmospheric Chemistry and Physics Discussions

absorption in a plane 4.2 m above the bottom of the AIDA chamber. The accuracy of the water vapor measurement is better than ±5 % (Fahey et al., 2014). The total water concentration (which is the sum of water vapor and the amount of condensed and frozen water contained in aerosol and/or cloud particles) was measured with a dew point mirror (373LX, MBW) by sampling air from the AIDA chamber via a heated stainless steel tube (accuracy ±3 %) By subtracting the gas phase water concentration from the total water concentration, the mass concentration of the condensed and frozen water can be calculated. The water vapor measurement by the AIDA TDL system has been compared with a range of other hygrometers during the AquaVIT-1 (intercomparison of atmospheric water vapor measurement techniques) campaign in 2007 and showed good agreement with established methods (Fahey et al., 2014). The ice saturation ratio, S_{ice}, in the AIDA chamber is calculated based on the gas temperature, the TDL water vapor measurements and the saturation vapor pressure over ice given by Murphy and Koop (2005).

For some experiments, in situ Fourier Transform Infrared spectroscopy (FTIR) was used to deduce the composition and mass concentration of the H_2SO_4/H_2O aerosol particles before and during expansion cooling (Wagner et al., 2008). Laser light scattering and depolarization measurements with the SIMONE instrument (Schnaiter et al., 2012) allowed for a precise determination of the freezing onset of the H_2SO_4/H_2O aerosol particles during expansion cooling, as described in Sect. 2.3. In the SIMONE set-up, a polarized laser beam with an emission wavelength of 488 nm is directed horizontally across the AIDA chamber. Photomultipliers detect the light scattered by the aerosol and/or cloud particles in the forward (2°) and backward (178°) direction. At 178°, the scattering intensities are measured polarization-resolved, enabling the determination of the back-scattering linear depolarization ratio, which is zero for the spherical H_2SO_4/H_2O solution droplets but increases as soon as aspherical ice crystals are formed after the freezing onset.

The number size distribution of aersosol and cloud particles was continuously measured by two optical particle counters (OPC; model: welas, Palas GmbH), which were sampling via a vertical line from the bottom of the AIDA vessel. The size classification and measurement ranges of the two OPCs (named welas1 and welas2) depend on the particle shape and refractive index. For example, for spherical particles with a refractive index of 1.33, the size ranges of the two sensors are 0.7 to 46 µm (welas1) and 5 to 240 µm (welas2). In Sect. 2.3, it is described how the OPC records are analyzed to provide a second measure for the freezing onset of the H_2SO_4/H_2O aerosol particles in addition to the SIMONE depolarization data.

2.2 Characterization of the H_2SO_4/H_2O aerosol particles

The H_2SO_4/H_2O aerosol particles were characterized after their injection into the AIDA chamber. A CPC continuously measured the number concentration of aerosol particles, $c_{aerosol}$ with diameters in the size from 10 nm up to 3 µm inside the chamber. The size distribution of the particles was measured two times after the injection by APS and SMPS. The SMPS detects aerosol particles in a size range between 0.014 and 0.82 µm (mobility diameter), whereas the APS only measures larger particles with diameters between 0.523 and 19.81 µm (aerodynamic diameter). As aqueous aerosol particles are spherical, the dynamic shape factor to convert the mobility diameter to a geometric diameter was set to unity. To transform the aerodynamic diameter to a geometric diameter, we applied the same shape factor together with the particle density, which was calculated with the E-AIM model for the specific equilibrium H_2SO_4/H_2O composition. The combination of APS und SMPS data provides particle size distributions over the whole relevant size range. For most of the experiments, the measured size distribution

https://doi.org/10.5194/acp-2021-319
Preprint. Discussion started: 21 April 2021


Atmospheric Chemistry and Physics Discussions

could be well described and fitted by an unimodal lognormal distribution with the parameters N (total number concentrations), D_m (median diameter) and σ (geometric standard deviation). Figure 2 shows the lognormal fits of the size distributions for all AIDA experiments for which APS/SMPS size distribution measurements were available. The median diameter ranges from about 30 nm to 1.1 µm. The measured size distribution of experiment number 14 of the ICE01 campaign (grey dots) shows the typically good agreement between the measurement and the lognormal fit. For several experiments with a start temperature below about 210 K, we observed continuously increasing aerosol particle concentrations in the CPC measurements after the H_2SO_4 aerosol injection had been stopped. The injected H_2SO_4 vapor further nucleated small aerosol particles in the cold environment in the AIDA chamber, creating a second mode in the number size distribution at diameters between 10 nm and 30 nm. As these nanometer-sized particles from the occasional second nucleation mode retain a higher solute concentration due to the Kelvin effect and have a lower freezing probability due to their small volume compared to the H_2SO_4/H_2O particles of diameters > 100 nm in the principal nucleation mode, they do not significantly contribute to the observed homogeneous ice nucleation modes during expansion cooling.

2.3 Determination of freezing onsets

The freezing onsets were determined based on ice crystal number concentration measurements by the OPCs and the depolarization ratio records by SIMONE. We illustrate our approach using the measured time series of experiment number 4 of the TROPIC04 campaign as an example, see Fig. 3. At time $t = 0$ the expansion started with pressure and temperature immediately decreasing (black and red lines, upper panel). The relative humidity with respect to ice computed for gas phase and total water increased accordingly (middle panel). The H_2SO_4/H_2O aerosol particles took up water in order to maintain thermodynamic equilibrium with the environment, which is visible in the faster increase in total water in comparison with the gas phase. This observation was supported by the SIMONE light scattering measurements (bottom panel), in which the forward scattering intensity (2°, dark red) also continuously increased with the beginning of expansion cooling, which is due to the increasing size of the aerosol particles due to the water uptake. The depolarization ratio (red), however, remained constant at the zero background level in this initial time period, which indicates that the particles still had a spherical shape, meaning they were in liquid phase. After about 280 s of pumping, a sharp increase was observed in the depolarization ratio, which is indicative for the formation of aspherical ice crystals in the chamber (red dashed line). The forward scattering signal also showed a strong increase at the same time because the nucleated ice crystals rapidly grow to large sizes with much higher scattering cross sections compared to the unactivated H_2SO_4/H_2O aerosol particles. A few seconds later, the activated fraction $N_{ice}/c_{aerosol}$, relating the number concentration of nucleated ice crystals, N_{ice}, to $c_{aerosol}$ from the CPC data, sharply increased, indicating the detection of ice particles in the OPC measurements (blue dashed line). The temperature and ice saturation ratio at the times derived in this way denoted the ice onset conditions T_{ice} and $S_{ice,fr}$.

For the derivation of N_{ice} from the OPC measurements, it was feasible for most experiments to define a specific optical threshold size to distinguish between smaller-sized H_2SO_4/H_2O aerosol particles and larger sized ice crystals. This procedure was applied to experiments at starting temperatures above about 200 K, where the ice crystals rapidly grew to much larger sizes in comparison to the aerosol population. The optical size threshold was typically set to values between 2 and 10 µm, depending

https://doi.org/10.5194/acp-2021-319
Preprint. Discussion started: 21 April 2021


Atmospheric Chemistry and Physics Discussions

on the aerosol particle size distribution. All particles larger than this size threshold were counted as ice, all smaller particles as H_2SO_4/H_2O aerosol particles. For experiments at temperatures below about 200 K, ice crystal growth is comparatively slow and the sizes are much smaller than those of ice crystals formed at higher temperatures. In these low temperature experiments, N_{ice} was therefore evaluated by analyzing the relative increase of the number concentrations in each size bin of the size distribution measurements instead of defining a size threshold. The ice number concentration and the resulting activated fraction derived from both methods show a sharp increase as soon as ice was formed, and we define the time of this sharp increase as the time of freezing onset. An estimate for the uncertainty of the freezing onset time is given in Sect. 2.4.

Regarding the SIMONE measurements, the onset of ice nucleation was defined as the start of the sharp increase in the back-scattering linear depolarization ratio and the overall back-scattering signals. As SIMONE measures the particle phase in situ, this method is not influenced by any possible artefacts induced by sampling. The time corresponding to the sharp increase of the depolarization ratio was evaluated visually from the individual experimental time series. Figure A1 shows a comparison of the ice onset conditions determined from the OPC and SIMONE measurements. Both the values for T_{ice} and $S_{ice,fr}$ agree well for all analyzed experiments, underlining the consistency between the SIMONE measurement, where the nucleated ice crystals are detected in situ in the AIDA chamber, and the OPC measurement, where the ice crystals are sampled from the chamber.

In general, the freezing onsets determined in the AIDA chamber are sensitive to nucleation rate coefficients between $J_V = 5 \cdot 10^8\,\mathrm{cm^3\,s^{-1}}$ and $J_V = 10^{13}\,\mathrm{cm^3\,s^{-1}}$, as reported in Möhler et al. (2003). These nucleation rate coefficients were determined for sulfuric acid aerosol particles with diameters between 0.5 and 2 µm with an estimated freezing probability between 0.02 and 0.5. The time delay for the detection of the nucleation peak ranged between 1 and 10 s (Möhler et al., 2003).

2.4 Analysis of uncertainties

In this Section, we will discuss the sources of uncertainties for the determination of the freezing onset conditions T_{ice} and $S_{ice,fr}$.

Regarding the freezing onset temperature T_{ice}, there are two major sources of uncertainties influencing its determination. The first source of uncertainty is related to the onset time determined from the OPC and SIMONE records, which is described in detail in Sect. 2.3. The comparison shown in Fig. A1 has illustrated that both methods to determine the freezing onset conditions agree very well. Moreover, given the steepness of the N_{ice} and depolarization ratio curves at the onset of ice nucleation, the experimental error in the determination of the freezing onset time is assumed to be small. We determined an uncertainty of ±3 s for the onset time. The variability of the gas temperature T in this 6 s time interval is a first factor contributing to the uncertainty of T_{ice}. The second source of uncertainty in the determination of T_{ice} is the temperature distribution inside the chamber. Five vertically and five horizontally distributed temperature sensors inside the AIDA chamber were considered to account for temperature inhomogeneity for each experiment. Prior to the experiment start, the deviation of the temperature measurements of all sensors is usually below 0.1 K. In the course of the experiment, the measured temperatures start to deviate. Especially the deviation in the vertical is increasing, whereas the horizontal deviation remains comparably small. Depending on the spread in vertical temperatures in the 6 s time interval around the freezing onset, we account for an additional uncertainty in T_{ice}. As the deviation of the temperature sensors at the time of freezing onset varies from experiment to experiment, the

https://doi.org/10.5194/acp-2021-319
Preprint. Discussion started: 21 April 2021


Atmospheric Chemistry and Physics Discussions

uncertainty for every single experiment were analyzed individually. A typical deviation at the time of the freezing is about $\pm 0.5\,\mathrm{K}$.

Regarding the ice saturation ratio at freezing onset $S_{ice,fr}$, there are three major sources contributing to the uncertainty in its determination. The first source is the uncertainty in the determination of the freezing onset time from OPC and SIMONE measurements, which is assumed to be $\pm 3\,\mathrm{s}$, as described above. For calculating $S_{ice,fr}$, the measured water vapor pressure p_w is divided by the water saturation vapor pressure with respect to ice $p_{sat,ice}(T)$. For $p_{sat,ice}$, the parameterization given by Murphy and Koop (2005) was used. As this parameterization depends on temperature, the temperature uncertainty including the temperature distribution inside the chamber in the time interval of 6 s affects the uncertainty of $S_{ice,fr}$ via this parameter and denotes the second factor contributing to the uncertainty in $S_{ice,fr}$. The third source of uncertainty is the direct measurement of p_w by the TDL hygrometer, with a general measurement accuracy of $\pm 5\,\%$. It is assumed that the TDL has a slight tendency to underestimate water vapor content at higher temperatures and to overestimate at lower temperatures ($T <$ about 220 K) (Fahey et al., 2014). For a reasonable correction of the TDL measurements especially at low temperatures, a specific time interval after pumping was stopped and a dense cloud persisted in the chamber was considered. During this time, the interior of the chamber is assumed to be saturated with respect to ice. We can therefore use this time period as a reference to correct our measurements to reasonable values. The highest correction factors were applied on the lowest temperature experiments, which resulted in a shift of up to 0.17 S_{ice} towards lower values. For the highest temperatures, the correction factor was often near zero or only a few percent. Finally, we account for the uncertainty in $S_{ice,fr}$ by considering the three sources of uncertainty individually determined for each experiment.

2.5 Overview of AIDA campaigns and experiments

All experiments evaluated for this work are listed in Table B1, together with the initial pressure, p_0, and temperature, T_0, before the start of the expansion, as well as the temperature and ice saturation ratio, T_{ice} and $S_{ice,fr}$, and the associated cooling rate, cr, and vertical velocity, v, at the derived homogeneous freezing onset. In Figure B1, six histograms show the range and frequency of experimental conditions for all considered AIDA experiments. Except for two experiments, all expansions were started at ambient pressure around 1000 hPa. Note that in the atmosphere, cirrus clouds are formed at much lower pressures. This, however, is not expected to be crucial for investigating the freezing onset conditions in terms of T and S_{ice}. With various start temperatures between 190 K and 236 K, our experiments cover a broad range of temperatures relevant for homogeneous freezing processes. Most of the experiments started between 210 K and 215 K, but with the series of TROPIC campaigns conducted in 2019 and 2020, we have significantly extended the data set at temperatures below 200 K. The majority of cooling rates determined at the associated freezing onset was around $1\,\mathrm{K\,min^{-1}}$, which corresponds to a vertical velocity of about $1.67\,\mathrm{m\,s^{-1}}$ assuming dry adiabatic conditions. Only a few particular experiments had higher cooling rates up to $5\,\mathrm{K\,min^{-1}}$ (about $8.33\,\mathrm{m\,s^{-1}}$). The injected H_2SO_4/H_2O aerosol particle population also covered a broad range of characteristic parameters with mean diameters between 30 nm and 1.1 µm and number concentrations from $30\,\mathrm{cm^{-3}}$ up to several $1000\,\mathrm{cm^{-3}}$. Finally, the weight percent composition of the H_2SO_4/H_2O solution particles, $wt\%$, at the beginning of each experiment ranged between 32 % and 41 %. As the aerosol particles are assumed to be in thermodynamic equilibrium with the environment before

https://doi.org/10.5194/acp-2021-319
Preprint. Discussion started: 21 April 2021


Atmospheric Chemistry and Physics Discussions

starting the expansion, the E-AIM model was used to calculate the equilibrium weight percent composition at the measured temperature and relative humidity conditions inside the chamber.

3 Results and Discussion

The homogeneous freezing onsets in AIDA were determined as described in Sect. 2.3 using the OPC ice count and SIMONE data. Figure 4 shows the freezing onsets color-coded for the respective AIDA campaign and the corresponding year. For comparison, the WAC-based temperature dependent Koop2000 homogeneous freezing onset lines for nucleation rate coefficients of $J_V = 5 \cdot 10^8\,\mathrm{cm^{-3}\,s^{-1}}$ (dotted line) and $J_V = 10^{13}\,\mathrm{cm^{-3}\,s^{-1}}$ (dashed line) are shown (Möhler et al., 2003), as well as the liquid water saturation ratios computed using the parameterization by Murphy and Koop (2005) (solid black line) and the more recent parameterization by Nachbar et al. (2019) (solid blue line). The latter is suggested to be used only for temperatures $T > 200\,\mathrm{K}$. We found that the homogeneous freezing onsets of H_2SO_4/H_2O particles at temperatures $T > 205\,\mathrm{K}$ agree within the measurement uncertainties to Koop2000. With decreasing temperature, the AIDA measurements show an increasing deviation from Koop2000 towards higher ice saturation ratios.

The Koop2000 lines are based on homogeneous freezing experiments of 18 different aqueous solutions with a known and constant composition. The homogeneous freezing temperature was measured as a function of the concentration of the solute. Converting the solute concentration into water activity resulted in a close match of the freezing temperatures for the different solutes. It was therefore suggested to formulate the freezing nucleation rate coefficients of aqueous solution particles only as function of the water activity and the temperature. In the present study, the homogeneous freezing of water with H_2SO_4 as the solute was measured as a function of the steady increase of the S_{ice} and the related increase of the water content or the dilution of the aerosol particles during the AIDA experiments. Thus, the observed differences of the AIDA homogeneous freezing onsets and the Koop2000 derived values may be related to the conversion of the water activity a_w of the solute used by Koop et al. (2000) to S_{ice} used in our studies as the basic water concentration unit in the aerosol system, or the assumption of thermodynamic equilibrium composition of the aerosol particles at the time of freezing onset.

Therefore, the measurement uncertainties of the water vapor concentration and the gas temperature are the first key aspect to discuss and interpret the AIDA data in comparison to Koop2000. In the present experiments, the water vapor concentration was directly measured in situ with a TDL setup (see Sect. 2.1) which was not yet available during the previous AIDA experiments (Möhler et al., 2003; Mangold et al., 2005). For the latter experiments, gas phase water concentration was derived from the total water measurements with the Lyman-α hygrometer FISH (Meyer et al., 2015) by subtracting the aerosol water content, which was calculated from the sulfuric acid aerosol mass concentration and the molar ratio of sulfuric acid and water in the aerosol particles at thermodynamic equilibrium composition (Möhler et al., 2003). The sulfuric acid mass concentration was determined by ion chromatography analysis of aerosol filter samples. The contribution of the aerosol water content to the total water content was below 1 % at temperatures around 235 K and increased to about 10 % at temperatures around 195 K. Therefore, this correction had only a minor contribution to the overall uncertainty of $S_{ice,fr}$, which varied between ± 0.08 and ± 0.13 (see Table 1 in (Möhler et al., 2003)). The uncertainty of the $S_{ice,fr}$ values derived in this manner varies from about

https://doi.org/10.5194/acp-2021-319
Preprint. Discussion started: 21 April 2021


Atmospheric Chemistry and Physics Discussions

± 0.06 at the higher temperatures to about ± 0.13 at the lower temperatures. Major contributions to this uncertainty come from the determination of the freezing onset time from OPC particle number and SIMONE scattering intensity and depolarization measurements, the direct measurements of the water vapor partial pressure, and the gas temperature uncertainty and chamber internal variability needed to calculate the water vapor saturation pressure with respect to the ice phase (see Sect. 2.4). Within these uncertainties, the two data sets from previous and more recent AIDA cloud simulation chamber experiments agree well with each other, and show both a clear trend of increasing freezing onsets to lower temperatures in comparison to Koop2000.

The second important aspect for discussing the deviation of AIDA freezing onsets from Koop2000 is the assumption of thermodynamic equilibrium composition of the aerosol particles in the dynamic environment of changing temperature and relative humidity during the AIDA experiments. The process modeling results by Haag et al. (2003) showed that larger aerosol particles may have a slightly enhanced sulfuric acid concentration, in particular during experiments at high cooling rates and low temperatures, but that the majority of smaller particles can well follow thermodynamic equilibrium in typical AIDA cloud expansion experiments. A similar result was obtained by Wagner et al. (2008) with a thorough analysis and application of the process model MAID (Bunz et al., 2008) for AIDA experiments with aqueous sulfuric acid aerosol particles performed at temperatures between 230 K and 205 K.

In order to support our assumption that the aerosol particles freezing in AIDA cloud expansion experiments are at or at least close to thermodynamic equilibrium conditions, we performed an experiment starting at a gas temperature of about 197 K, as shown in Fig. 5. This experiment was not performed with a constant pump rate as all other experiments discussed here, but with an intermediate reduction of the pump rate in order to maintain a constant relative humidity for a longer time period. The experiment was started as other experiments with decreasing temperature and increasing relative humidity, but after the relative humidity passed the Koop2000 line after about 80 s, the pump rate was reduced to keep the relative humidity at an almost constant value above the Koop2000 line for about five minutes to give the particles enough time for reaching thermodynamic equilibrium. The forward scattering intensity of the SIMONE measurements (dark red) shows a clear increase at the beginning of the experiments, indicating the growing of the aerosol particles due to water uptake with increasing relative humidity. As soon as the relative humidity is kept at a constant value, no further increase in the forward scattering intensity was observed. This supports our assumption that the aerosol particles can well follow thermodynamic equilibrium conditions during an AIDA experiment at typical pump rates and related rates of cooling and relative humidity increase. As soon as the pump rate was increased again at about 450 s experiment time, the freezing onset was observed at a relative humidity similar to other experiments with constant pump rate. The fact that no ice formation was observed during the long time period with almost constant relative humidity well above the Koop2000 line supports our assumption, that the observed shift of the freezing onset to higher relative humidity is not caused by a delayed nucleation due to kinetic limitation of water diffusion to and uptake by the aerosol particles. The result of this experiment also indicates that the observed high freezing onsets may not be caused by a delayed growth of the pristine ice nucleus embedded in a highly concentrated solution layer as suggested in previous studies (Clapp et al., 1997; Bogdan et al., 2006; Bogdan, 2006; Bogdan and Molina, 2010; Bogdan et al., 2013).

Results from Wagner et al. (2008) and more recent measurements during the TROPIC04 campaign show that the mass fraction of sulfuric acid in the H_2SO_4/H_2O particles measured by FTIR extinction spectroscopy right before the homogeneous

https://doi.org/10.5194/acp-2021-319
Preprint. Discussion started: 21 April 2021


Atmospheric Chemistry and Physics Discussions

freezing onset tend to be slightly lower when compared to the composition of the freezing solutions shown in Koop et al. (2000), but still overlap in the range of uncertainties. This observation supports the assumption that the conversion from the $wt\%$-T-space into the S_{ice}-T-space is a potential explanation for the observed deviation to Koop2000. For this conversion, the water vapor saturation pressure with respect to the supercooled liquid water phase is needed, or more precisely, the ratio of the saturation pressures with respect to the supercooled liquid and ice phases. The descriptions for the liquid water saturation pressures are rather uncertain, and various parameterizations deviate from each other (e.g. Buck, 1981; Sonntag, 1994; Tabazadeh et al., 1997; Murphy and Koop, 2005; Nachbar et al., 2019). In this work, we are using parameterizations from Murphy and Koop (2005) to calculate both liquid water and ice saturation pressures, but in a recent study Nachbar et al. (2019) suggested a new parameterization for liquid water saturation conditions which indicates that Murphy and Koop (2005) may increasingly underestimate the liquid water saturation pressure with decreasing temperature below about 220 K. Jensen et al. (2005) discussed that a shift of the liquid water saturation line to higher ice saturation ratios would also shift the homogeneous freezing onset in cirrus formation processes to higher ice saturation ratios. Higher liquid water saturation pressures would also reduce the difference between the AIDA and the Koop2000 freezing onsets for aqueous sulfuric acid aerosol particles.

Based on the AIDA results and the discussion above, we suggest a new parameterization for homogeneous freezing depending solely on S_{ice} and T. When plotted the SIMONE and OPC freezing onsets in an Arrhenius type diagram as $\ln(S_{ice})$ versus $1/T$ in Fig. 6a, the AIDA freezing onsets almost follow a straight line. Using an ordinary least square fit routine the data points are fitted by

$$\ln(S_{ice}) = a + b \cdot \frac{1}{T} \tag{1}$$

with fitting coefficients a and b. The coefficients of the fit shown in Fig. 6a are $a = -1.4 \pm 0.05$ and $b = 390 \pm 10$ K. This fit transferred into the S_{ice}-T-space and compared to Koop2000 and the water saturation lines is shown in 6b (grey line) with the range of fit uncertainty (grey shaded area). The goodness of fit is $R^2 = 0.92$. In a next step, this fit is constrained to the well-known homogeneous freezing temperature of pure water droplets, so that when applied to atmospheric models it matches the freezing point of pure water droplets (see Fig. 6c and d, red line). The fit was fixed to a temperature of 235 K and $S_{ice} = 1.45$, which is the point of water saturated conditions according to the parameterizations of Murphy and Koop (2005). This point corresponds to a nucleation rate coefficient of about $J_V = 4.5 \cdot 10^{10}\,\mathrm{cm^{-3}\,s^{-1}}$ according to the parameterization of Koop et al. (2000) for the nucleation rate coefficient in dependence on the temperature ($T = 235$ K) and water activity ($a_w = 1$ for pure water). This nucleation rate coefficient is in the range the AIDA experiments are sensitive to ($J_V = 5 \cdot 10^8$ to $10^{13}\,\mathrm{cm^{-3}\,s^{-1}}$) (Möhler et al., 2003). The coefficients of the constrained fit are $a = -0.75 \pm 0.04$ and $b = 263 \pm 8$ K. The goodness of the fit is also $R^2 = 0.92$. We suggest to use the constraint fit with the coefficients $a = -0.75 \pm 0.04$ and $b = 263 \pm 8$ K (see Eq. 1 and 6c and d, red line) for use in atmospheric models. This would then result in a shift of the homogeneous freezing onset in cirrus formation to ice saturation ratios of about 2.0 at temperatures around 185 K. A higher homogeneous freezing onset may also contribute to explain high ice saturation ratios reported for low temperatures in the upper troposphere in some field studies (Jensen et al., 2005; Lawson et al., 2008; Krämer et al., 2009; Krämer et al., 2020).

https://doi.org/10.5194/acp-2021-319
Preprint. Discussion started: 21 April 2021


Atmospheric Chemistry and Physics Discussions

4 Conclusions

In this study, we present and discuss a comprehensive set of homogeneous freezing measurements for H_2SO_4/H_2O aerosol particles. The experiments were conducted at the AIDA cloud simulation chamber and covered a wide range of temperatures, cooling rates, aerosol sizes and number concentrations. At temperatures above 205 K, the measured ice saturation ratios at homogeneous freezing onset $S_{ice,fr}$ agree with the water activity criterion (WAC) based predictions by Koop et al. (2000). Towards lower temperatures, however, the AIDA homogeneous freezing onset results show an increasing deviation from Koop2000 towards higher ice saturation ratios. For temperatures between 205 K and 185 K, the WAC-based ice saturation ratios increase from about 1.6 to 1.7, whereas the AIDA measurements show an increase from about 1.7 to about 2.0 in the same temperature range.

For the comparison with Koop2000, we assume the aerosol particles to be in thermodynamic equilibrium at freezing onset. This assumption is justified by previous measurements and process model results (Haag et al., 2003; Wagner et al., 2008). We also demonstrate that the enhanced freezing onset is not caused by a delayed water uptake and by that a delayed dilution during the AIDA experiments with steady increase of S_{ice}. For this we conducted an AIDA experiment during which S_{ice} was kept at an almost constant value well above the Koop2000 line for about 5 minutes. No ice formation or further water uptake of the aerosol particles was observed during this time period, but when increasing S_{ice} in the cloud chamber to higher values, the freezing onset occurred in agreement to results from experiments with steady increase of S_{ice}.

Further, the water activities a_w used by Koop2000 have to be converted into S_{ice} directly measured during AIDA experiments for comparing AIDA results with Koop2000. This conversion requires a formulation for the saturation vapor pressures over supercooled liquid water $p_{sat,liq}$, which are rather uncertain at low temperatures (Murphy and Koop, 2005). A recent study by Nachbar et al. (2019) suggested a new parameterization for $p_{sat,liq}$, which, for temperatures below about 220 K, increasingly deviates from Murphy and Koop (2005) to higher values with decreasing temperature. Higher $p_{sat,liq}$ would shift the Koop2000 freezing onsets to higher ice saturation ratios and would therefore reduce the difference between the AIDA and the Koop2000 freezing onsets. It was already discussed in Jensen et al. (2005) that a shift of the $p_{sat,liq}$ line to higher ice saturation ratios would also shift the homogeneous freezing onset in cirrus cloud formation processes to higher ice saturation ratios. A higher homogeneous freezing onset as derived from our experiments may also explain field observations of high clear-sky supersaturation, which should not occur according to the freezing thresholds predicted by Koop2000 (Jensen et al., 2005; Lawson et al., 2008; Krämer et al., 2009; Krämer et al., 2020).

We suggest a new parameterization for the homogeneous freezing onset of H_2SO_4/H_2O aerosol particles, which is based on an empirical fit to the AIDA results with the form $\ln(S_{ice}) = a + \frac{1}{T} \cdot b$ with fit parameters $a = -0.75 \pm 0.04$ and $b = 263 \pm 8$ K. This fit is constrained to the homogeneous freezing temperature of pure water at 235 K and water saturated conditions at this temperature. As homogeneously formed cirrus clouds usually have a higher optical depth due to higher ice crystal number concentrations and ice water content, the reflectivity of solar radiation is increased in comparison to heterogeneously formed cirrus (Lohmann et al., 2016). However, homogeneously formed cirrus clouds also reduce the outgoing longwave radiation (OLR) from below to be emitted in space due to their higher optical depth (Lohmann et al., 2016). Consequently, a precise

https://doi.org/10.5194/acp-2021-319
Preprint. Discussion started: 21 April 2021


Atmospheric Chemistry and Physics Discussions

description of homogeneous freezing processes is crucial to understand cloud radiative effects in the present climate as well as in predictions of climate change. The new parameterization suggested here may be used as a replacement of the Koop2000 homogeneous freezing onset lines. This may in particular be relevant for cirrus clouds in the cold tropical tropopause layer (TTL). TTL cirrus clouds have the highest occurrence frequency globally and the strongest radiative warming effect, which enhances their importance for the Earth's climate. The higher homogeneous freezing onsets would suppress the TTL cirrus cloud formation resulting in a decreasing cloud fraction (Jensen et al., 2005; Schoeberl et al., 2016), which would influence the global radiation budget by impacting the OLR (Mitchell and Finnegan, 2009) and reflected shortwave solar radiation.

Besides radiative effects, the presence of cirrus clouds in the tropopause region, especially in the TTL, are assumed to influence the water vapor mass flux from the troposphere to the stratosphere (Jensen et al., 1996; Hartmann et al., 2001; Corti et al., 2006). Air passing the TTL is dehydrated by crossing the cold point in the tropopause layer (Brewer, 1949), which then controls the stratospheric water vapor (Dinh and Fueglistaler, 2014). The supersaturations measured above the cold point tropopause suggest that the water exchange with the stratosphere is $10-20\,\%$ higher than expected (Rollins et al., 2016; Krämer et al., 2020), which might also be related to an enhanced freezing threshold (Schoeberl et al., 2016). To understand stratospheric water contents and related stratospheric chemistry, cirrus formation thresholds (Schoeberl et al., 2016), supersaturations and temperatures (Randel and Jensen, 2013; Randel and Park, 2019) in the tropopause region are of particular importance. Several studies have investigated the relation between the amount of stratospheric water vapor and the properties of the TTL in climate change scenarios (Solomon et al., 2010; Riese et al., 2012; Randel and Jensen, 2013), which puts the importance of upper tropospheric cirrus formation parameterizations into a larger context.

Ongoing experiments in the AIDA cloud simulation chamber aim at investigating homogeneous freezing onsets of different solutes and at constraining the descriptions for liquid water saturation pressures to experimental results.

Data availability. The measurement data shown in this study are available via the KITopen data repository under https://doi.org/10.5445/IR/1000130863 (Schneider et al., 2021)

Author contributions. JS wrote this paper supported by OM, KH and RW. OM, SB, KH, RW, HS, MS, TS, IS and JS planned and conducted the experiments at the AIDA chamber and did the analysis and interpretation of the respective measurement data. MK, MB, CR and TL contributed to the discussion and the interpretation of the data.

Competing interests. The authors declare no competing interests.

Acknowledgements. We thank all the members of the AIDA staff for their continuous support during the measurement campaigns. This work has been funded by the Deutsche Forschungsgemeinschaft (DFG) through several projects in the years since 2007 (AIDA-HALO

https://doi.org/10.5194/acp-2021-319
Preprint. Discussion started: 21 April 2021

Atmospheric Chemistry and Physics Discussions

projects 47366677 within the HALO priority program SPP-1294, WaterIsotopes project 181901664, project 170852269 within the research unit INUIT FOR 1525, AWiCiT project 311095914, PIRE TropiC project 392369854). We would also like to thank the Gutenberg Research College of the University of Mainz and the Carl Zeiss Foundation for support of this project. We acknowledge support by the KIT-Publication Fund of the Karlsruhe Institute of Technology.

https://doi.org/10.5194/acp-2021-319
Preprint. Discussion started: 21 April 2021

Atmospheric Chemistry and Physics Discussions

References

Benz, S., Megahed, K., Möhler, O., Saathoff, H., Wagner, R., and Schurath, U.: T-dependent rate measurements of homogeneous ice nucleation in cloud droplets using a large atmospheric simulation chamber, J. Photochem. Photobiol. A Chem., 176, 208–217, https://doi.org/10.1016/j.jphotochem.2005.08.026, 2005.

Bertram, A. K., Patterson, D. D., and Sloan, J. J.: Mechanisms and temperatures for the freezing of sulfuric acid aerosols measured by FTIR extinction spectroscopy, J. Phys. Chem., 100, 2376–2383, https://doi.org/10.1021/jp952551v, 1996.

Beyer, K. D., Seago, S. W., Chang, H. Y., and Molina, M. J.: Composition and freezing of aqueous H_2SO_4/HNO_3 solutions under polar stratospheric conditions, Geophys. Res. Lett., 21, 871–874, https://doi.org/10.1029/94GL00915, 1994.

Bogdan, A.: Reversible formation of glassy water in slowly cooling diluted drops, J. Phys. Chem. B, 110, 12 205–12 206, https://doi.org/10.1021/jp062464a, 2006.

Bogdan, A. and Molina, M. J.: Aqueous aerosol may build up an elevated upper tropospheric ice supersaturation and form mixed-phase particles after freezing, J. Phys. Chem. A, 114, 2821–2829, https://doi.org/10.1021/jp9086656, 2010.

Bogdan, A., Molina, M. J., Sassen, K., and Kulmala, M.: Formation of low-temperature cirrus from H_2SO_4/H_2O aerosol droplets, J. Phys. Chem. A, 110, 12 541–12 542, https://doi.org/10.1021/jp065898e, 2006.

Bogdan, A., Molina, M. J., Kulmala, M., Tenhu, H., and Loerting, T.: Solution coating around ice particles of incipient cirrus clouds, Proc. Natl. Acad. Sci. U. S. A., 110, E2439–E2439, https://doi.org/10.1073/pnas.1304471110, 2013.

Brewer, A. W.: Evidence for a world circulation provided by the measurements of helium and water vapour distribution in the stratosphere, Q. J. R. Meteorol. Soc., 75, 351–363, https://doi.org/10.1002/qj.49707532603, 1949.

Buck, A. L.: New equations for computing vapour pressure and enhancement factor., J. Appl. Meteorol., 20, 1527–1532, https://doi.org/10.1175/1520-0450(1981)020<1527:nefcvp>2.0.co;2, 1981.

Bunz, H., Benz, S., Gensch, I., and Krämer, M.: MAID: a model to simulate UT/LS aerosols and ice clouds, Environ. Res. Lett., 3, 035 001, https://doi.org/10.1088/1748-9326/3/3/035001, 2008.

Carslaw, K. S., Clegg, S. L., and Brimblecombe, P.: A thermodynamic model of the system HCl-HNO_3-H_2SO_4-H_2O, including solubilities of HBr, from <200 to 328 K, J. Phys. Chem., 99, 11 557–11 574, https://doi.org/10.1021/j100029a039, 1995.

Clapp, M. L., Niedziela, R. F., Richwine, L. J., Dransfield, T., Miller, R. E., and Worsnop, D. R.: Infrared spectroscopy of sulfuric acid/water aerosols: Freezing characteristics, J. Geophys. Res. Atmos., 102, 8899–8907, https://doi.org/10.1029/97jd00012, 1997.

Clegg, S. L. and Brimblecombe, P.: Application of a Multicomponent Thermodynamic Model to Activities and Thermal Properties of 0–40 mol kg−1 Aqueous Sulfuric Acid from <200 to 328 K, J. Chem. Eng. Data, 40, 43–64, https://doi.org/10.1021/je00017a012, 1995.

Corti, T., Luo, B. P., Fu, Q., Vömel, H., and Peter, T.: The impact of cirrus clouds on tropical troposphere-to-stratosphere transport, Atmos. Chem. Phys. Discuss, 6, 2539–2547, https://doi.org/10.5194/acp-6-2539-2006, 2006.

Cziczo, D. J. and Froyd, K. D.: Sampling the composition of cirrus ice residuals, Atmos. Res., 142, 15–31, https://doi.org/10.1016/j.atmosres.2013.06.012, 2014.

Cziczo, D. J., Froyd, K. D., Hoose, C., Jensen, E. J., Diao, M., Zondlo, M. A., Smith, J. B., Twohy, C. H., and Murphy, D. M.: Clarifying the dominant sources and mechanisms of cirrus cloud formation, Science (80-.)., 340, 1320–1324, https://doi.org/10.1126/science.1234145, 2013.

Dinh, T. and Fueglistaler, S.: Microphysical, radiative, and dynamical impacts of thin cirrus clouds on humidity in the tropical tropopause layer and lower stratosphere, Geophys. Res. Lett., 41, 6949–6955, https://doi.org/10.1002/2014GL061289, 2014.

https://doi.org/10.5194/acp-2021-319
Preprint. Discussion started: 21 April 2021

Atmospheric Chemistry and Physics Discussions

Fahey, D. W., Gao, R. S., Möhler, O., Saathoff, H., Schiller, C., Ebert, V., Krämer, M., Peter, T., Amarouche, N., Avallone, L. M., Bauer, R., Bozóki, Z., Christensen, L. E., Davis, S. M., Durry, G., Dyroff, C., Herman, R. L., Hunsmann, S., Khaykin, S. M., Mackrodt, P., Meyer, J., Smith, J. B., Spelten, N., Troy, R. F., Vömel, H., Wagner, S., and Wienhold, F. G.: The AquaVIT-1 intercomparison of atmospheric water vapor measurement techniques, Atmos. Meas. Tech., 7, 3177–3213, https://doi.org/10.5194/amt-7-3177-2014, 2014.

Haag, W., Kärcher, B., Schaefers, S., Stetzer, O., Möhler, O., Schurath, U., Krämer, M., and Schiller, C.: Numerical simulations of homogeneous freezing processes in the aerosol chamber AIDA, Atmos. Chem. Phys., 3, 195–210, https://doi.org/10.5194/acp-3-195-2003, 2003.

Hartmann, D. L., Holton, J. R., and Fu, Q.: The heat balance of the tropical tropopause, cirrus and stratospheric dehydration, Geophys. Res. Lett., 28, 1969–1972, https://doi.org/10.1029/2000GL012833, 2001.

Jensen, E. J., Toon, O. B., Pfister, L., and Selkirk, H. B.: Dehydration of the upper troposphere and lower stratosphere by subvisible cirrus clouds near the tropical tropopause, Geophys. Res. Lett., 23, 825–828, https://doi.org/10.1029/96GL00722, 1996.

Jensen, E. J., Smith, J. B., Pfister, L., Pittman, J. V., Weinstock, E. M., Sayres, D. S., Herman, R. L., Troy, R. F., Rosenlof, K., Thompson, T. L., Fridlind, A. M., Hudson, P. K., Cziczo, D. J., Heymsfield, A. J., Schmitt, C., and Wilson, J. C.: Ice supersaturations exceeding 100% at the cold tropical tropopause: Implications for cirrus formation and dehydration, Atmos. Chem. Phys., 5, 851–862, https://doi.org/10.5194/acp-5-851-2005, 2005.

Koop, T.: Atmospheric Water, in: Water: Fundamentals as the Basis for Understanding the Environment and Promoting Technology, edited by Debenedetti, P. G., Ricci, A., and Bruni, F., pp. 45–75, IOS, Amsterdam, Bologna, https://doi.org/10.3254/978-1-61499-507-4-45, 2015.

Koop, T., Luo, B., Tsias, A., and Peter, T.: Water activity as the determinant for homogeneous ice nucleation in aqueous solutions, Nature, 406, 611–614, https://doi.org/10.1038/35020537, 2000.

Krämer, M., Schiller, C., Afchine, A., Bauer, R., Gensch, I., Mangold, A., Schlicht, S., Spelten, N., Sitnikov, N., Borrmann, S., De Reus, M., and Spichtinger, P.: Ice supersaturations and cirrus cloud crystal numbers, Atmos. Chem. Phys., 9, 3505–3522, https://doi.org/10.5194/acp-9-3505-2009, 2009.

Krämer, M., Rolf, C., Spelten, N., Afchine, A., Fahey, D., Jensen, E., Khaykin, S., Kuhn, T., Lawson, P., Lykov, A., Pan, L. L., Riese, M., Rollins, A., Stroh, F., Thornberry, T., Wolf, V., Woods, S., Spichtinger, P., Quaas, J., and Sourdeval, O.: A microphysics guide to cirrus – Part 2: Climatologies of clouds and humidity from observations, Atmos. Chem. Phys., 20, 12 569–12 608, https://doi.org/10.5194/acp-20-12569-2020, 2020.

Lawson, R. P., Pilson, B., Baker, B., Mo, Q., Jensen, E., Pfister, L., and Bui, P.: Aircraft measurements of microphysical properties of subvisible cirrus in the tropical tropopause layer, Atmos. Chem. Phys., 8, 1609–1620, https://doi.org/10.5194/acp-8-1609-2008, 2008.

Lohmann, U., Lüönd, F., and Mahrt, F.: An introduction to clouds: From the microscale to climate, Cambridge University Press, 2016.

Lynch, D.: Cirrus, Oxford University Press, Oxford, 2002.

Malkin, T. L., Murray, B. J., Brukhno, A. V., Anwar, J., and Salzmann, C. G.: Structure of ice crystallized from supercooled water, Proc. Natl. Acad. Sci. U. S. A., 109, 1041–1045, https://doi.org/10.1073/pnas.1113059109, 2012.

Mangold, A., Wagner, R., Saathoff, H., Schurath, U., Giesemann, C., Ebert, V., Krämer, M., and Möhler, O.: Experimental investigation of ice nucleation by different types of aerosols in the aerosol chamber AIDA: Implications to microphysics of cirrus clouds, Meteorol. Zeitschrift, 14, 485–497, https://doi.org/10.1127/0941-2948/2005/0053, 2005.

Meyer, J., Rolf, C., Schiller, C., Rohs, S., Spelten, N., Afchine, A., Zöger, M., Sitnikov, N., Thornberry, T. D., Rollins, A. W., Bozóki, Z., Tátrai, D., Ebert, V., Kühnreich, B., Mackrodt, P., Möhler, O., Saathoff, H., Rosenlof, K. H., and Krämer, M.: Two decades of water vapor

https://doi.org/10.5194/acp-2021-319
Preprint. Discussion started: 21 April 2021

Atmospheric Chemistry and Physics Discussions

measurements with the FISH fluorescence hygrometer: a review, Atmos. Chem. Phys., 15, 8521–8538, https://doi.org/10.5194/acp-15-8521-2015, 2015.

Mitchell, D. L. and Finnegan, W.: Modification of cirrus clouds to reduce global warming, Environ. Res. Lett., 4, 045 102, https://doi.org/10.1088/1748-9326/4/4/045102, 2009.

Möhler, O., Stetzer, O., Schaefers, S., Linke, C., Schnaiter, M., Tiede, R., Saathoff, H., Krämer, M., Mangold, A., Budz, P., Zink, P., Schreiner, J., Mauersberger, K., Haag, W., Kärcher, B., and Schurath, U.: Experimental investigation of homogeneous freezing of sulphuric acid particles in the aerosol chamber AIDA, Atmos. Chem. Phys., 3, 211–223, https://doi.org/10.5194/acp-3-211-2003, 2003.

Murphy, D. M. and Koop, T.: Review of the vapour pressures of ice and supercooled water for atmospheric applications, Q. J. R. Meteorol. Soc., 131, 1539–1565, https://doi.org/10.1256/qj.04.94, 2005.

Nachbar, M., Duft, D., and Leisner, T.: The vapor pressure of liquid and solid water phases at conditions relevant to the atmosphere, J. Chem. Phys., 151, 064 504, https://doi.org/10.1063/1.5100364, 2019.

Ohtake, T.: Freezing points of H_2SO_4 aqueous solutions and formation of stratospheric ice clouds, Tellus B, 45, 138–144, https://doi.org/10.1034/j.1600-0889.1993.t01-1-00006.x, 1993.

Randel, W. and Park, M.: Diagnosing observed stratospheric water vapor relationships to the cold point tropical tropopause, J. Geophys. Res. Atmos., 124, 2019JD030 648, https://doi.org/10.1029/2019JD030648, 2019.

Randel, W. J. and Jensen, E. J.: Physical processes in the tropical tropopause layer and their roles in a changing climate, Nat. Geosci., 6, 169–176, https://doi.org/10.1038/ngeo1733, 2013.

Riese, M., Ploeger, F., Rap, A., Vogel, B., Konopka, P., Dameris, M., and Forster, P.: Impact of uncertainties in atmospheric mixing on simulated UTLS composition and related radiative effects, J. Geophys. Res., 117, https://doi.org/10.1029/2012JD017751, 2012.

Rollins, A., Thornberry, T., Gao, R., Woods, S., Lawson, R., Bui, T., Jensen, E., and Fahey, D.: Observational constraints on the efficiency of dehydration mechanisms in the tropical tropopause layer, Geophys. Res. Lett., 43, 2912–2918, https://doi.org/10.1002/2016GL067972, 2016.

Russo, J., Romano, F., and Tanaka, H.: New metastable form of ice and its role in the homogeneous crystallization of water, Nat. Mater., 13, 733–739, https://doi.org/10.1038/nmat3977, 2014.

Schnaiter, M., Büttner, S., Möhler, O., Skrotzki, J., Vragel, M., and Wagner, R.: Influence of particle size and shape on the backscattering linear depolarisation ratio of small ice crystals-cloud chamber measurements in the context of contrail and cirrus microphysics, Atmos. Chem. Phys., 12, 10 465–10 484, https://doi.org/10.5194/acp-12-10465-2012, 2012.

Schneider, J., Höhler, K., Wagner, R., Saathoff, H., Schnaiter, M., Schorr, T., Steinke, I., Benz, S., Baumgartner, M., Rolf, C., Krämer, M., Leisner, T., and Möhler, O.: Datasets to: High Homogeneous Freezing Onsets of Sulfuric Acid Aerosol at Cirrus Temperatures, KITOpen [data set], https://doi.org/10.5445/IR/1000130863, 2021.

Schoeberl, M., Dessler, A., Ye, H., Wang, T., Avery, M., and Jensen, E.: The impact of gravity waves and cloud nucleation threshold on stratospheric water and tropical tropospheric cloud fraction, Earth Sp. Sci., 3, 295–305, https://doi.org/10.1002/2016EA000180, 2016.

Shafique, U., Anwar, J., Ali Munawar, M., uz Zaman, W., Rehman, R., Dar, A., Salman, M., Saleem, M., Shahid, N., Akram, M., Naseer, A., and Jamil, N.: Chemistry of ice: Migration of ions and gases by directional freezing of water, Arab. J. Chem., 9, S47 – S53, https://doi.org/https://doi.org/10.1016/j.arabjc.2011.02.019, 2016.

Solomon, S., Rosenlof, K. H., Portmann, R. W., Daniel, J. S., Davis, S. M., Sanford, T. J., and Plattner, G. K.: Contributions of stratospheric water vapor to decadal changes in the rate of global warming, Science (80-.)., 327, 1219–1223, https://doi.org/10.1126/science.1182488, 2010.

https://doi.org/10.5194/acp-2021-319
Preprint. Discussion started: 21 April 2021

Atmospheric Chemistry and Physics Discussions

Song, N.: Freezing temperatures of H2SO4/HNO3/H2O mixtures: Implications for polar stratospheric clouds, Geophys. Res. Lett., 21, 2709–2712, https://doi.org/10.1029/94GL02459, 1994.

Sonntag, D.: Advancements in the field of hygrometry, Meteorol. Zeitschrift, 3, 51–66, https://doi.org/10.1127/metz/3/1994/51, 1994.

Tabazadeh, A., Toon, O. B., Clegg, S. L., and Hamill, P.: A new parameterization of H_2SO_4/H_2O aerosol composition: Atmospheric implications, Geophys. Res. Lett., 24, 1931–1934, https://doi.org/10.1029/97GL01879, 1997.

Wagner, R., Benz, S., Bunz, H., Möhler, O., Saathoff, H., Schnaiter, M., Leisner, T., and Ebert, V.: Infrared optical constants of highly diluted sulfuric acid solution droplets at cirrus temperatures, J. Phys. Chem. A, 112, 11 661–11 676, https://doi.org/10.1021/jp8066102, 2008.

Wagner, R., Linke, C., Naumann, K. H., Schnaiter, M., Vragel, M., Gangl, M., and Horvath, H.: A review of optical measurements at the aerosol and cloud chamber AIDA, J. Quant. Spectrosc. Radiat. Transf., 110, 930–949, https://doi.org/10.1016/j.jqsrt.2009.01.026, 2009.

Wexler, A. S. and Clegg, S. L.: Atmospheric aerosol models for systems including the ions H^+, NH_4^+, Na^+, SO_4^{2-}, NO_3^-, Cl^-, Br^-, and H_2O, J. Geophys. Res. Atmos., 107, https://doi.org/10.1029/2001JD000451, 2002.

https://doi.org/10.5194/acp-2021-319
Preprint. Discussion started: 21 April 2021

Atmospheric Chemistry and Physics Discussions

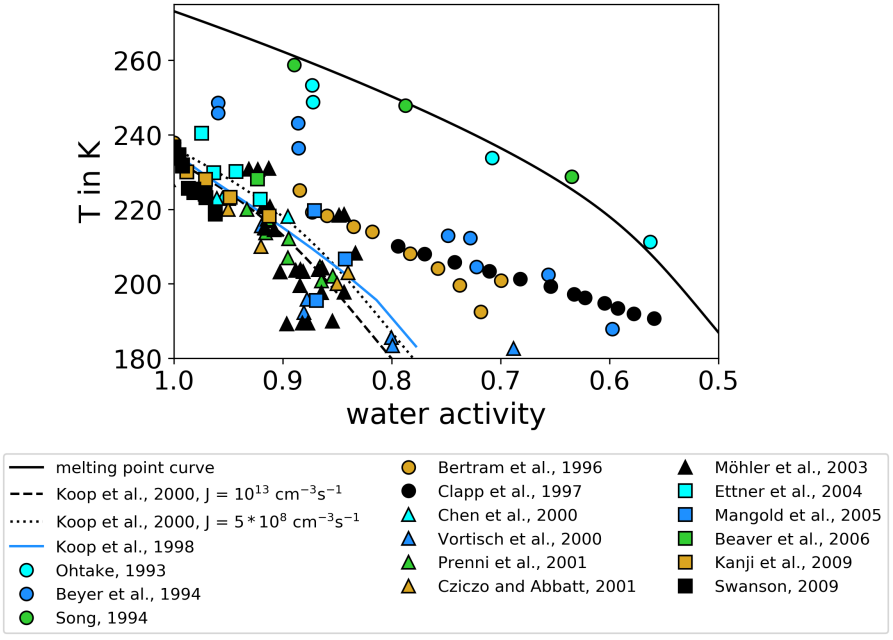

Figure 1. Review of homogeneous freezing measurements of H_2SO_4/H_2O solutions. The homogeneous freezing onsets of sulfuric acid solution samples reported in different studies are shown and compared. Most of the studies report onset temperatures and weight percentage of H_2SO_4 in the solution samples. We used the E-AIM model to transfer this weight percentage data into water activity, which is assumed to be equal to the relative humidity (assumption of thermodynamic equilibrium). If ice saturation ratios were given, the parameterizations of Murphy and Koop (2005) for the saturation pressures of supercooled liquid water and ice were used to calculate water activities. Additionally, the melting point line according to Murphy and Koop (2005) (solid line) and the homogeneous freezing thresholds for two different nucleation rate coefficients according to Koop et al. (2000) (dashed and dotted lines) are shown.

https://doi.org/10.5194/acp-2021-319
Preprint. Discussion started: 21 April 2021

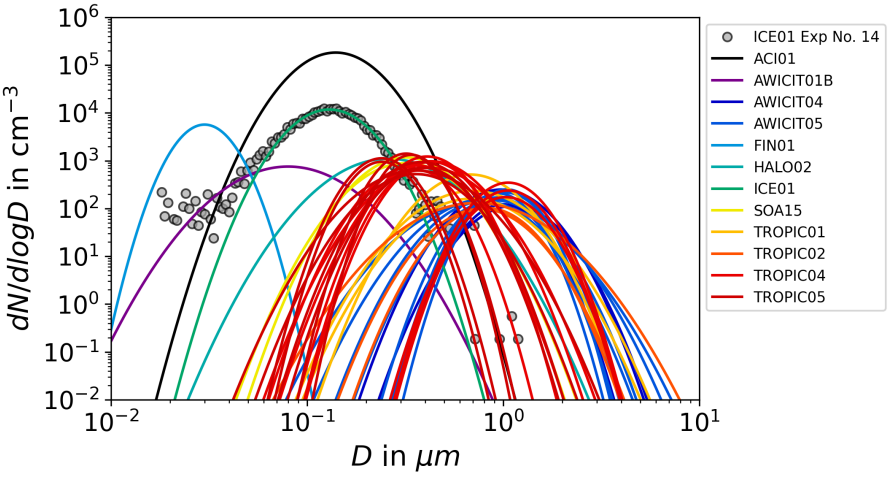

Figure 2. Number size distributions of H_2SO_4/H_2O aerosol particles. We show lognormal fitted number size distributions for all AIDA experiments for which size information is available. The grey dots show an exemplary size distribution showing that a longnormal fit generally is adequate to accurately represent the measured size distribution (for details see Sect. 2.2).

https://doi.org/10.5194/acp-2021-319
Preprint. Discussion started: 21 April 2021

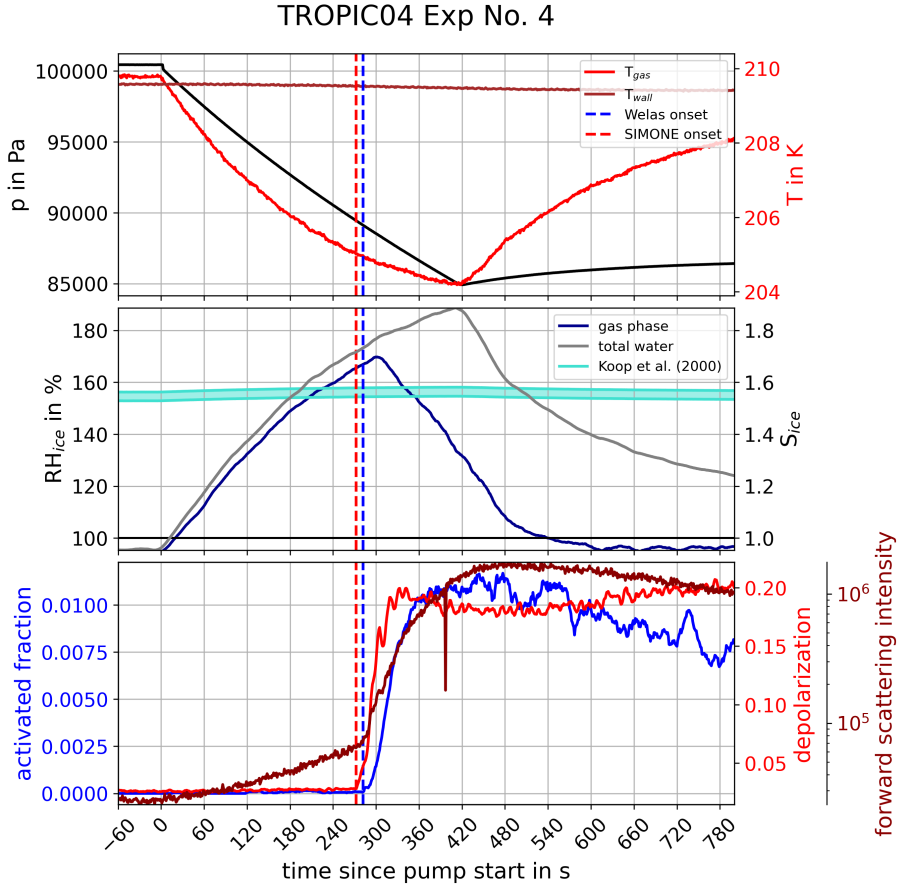

Figure 3. Time series of a typical AIDA homogeneous freezing experiment. The upper panel shows the course of pressure (black), as well as gas (red) and wall (dark red) temperature inside the AIDA chamber in dependence on the time since pump start at $t = 0$. Accordingly, the middle panel shows the course of relative humidity with respect to ice RH_{ice} and ice saturation ratio S_{ice} of gas phase (blue) and total water (grey). The turquoise area marks the range of freezing onset saturation ratios according to Koop et al. (2000). In the lower panel, the activated fraction of H_2SO_4/H_2O particles determined by OPC data (blue) and the forward scattering intensity (dark red) as well as the back-scattering depolarization ratio (red) derived from SIMONE light scattering measurements are presented. The time of homogeneous freezing onsets derived from the activated fraction (blue) and from the SIMONE measurements (red) are marked by the vertical dashed lines.

https://doi.org/10.5194/acp-2021-319
Preprint. Discussion started: 21 April 2021

Atmospheric Chemistry and Physics Discussions

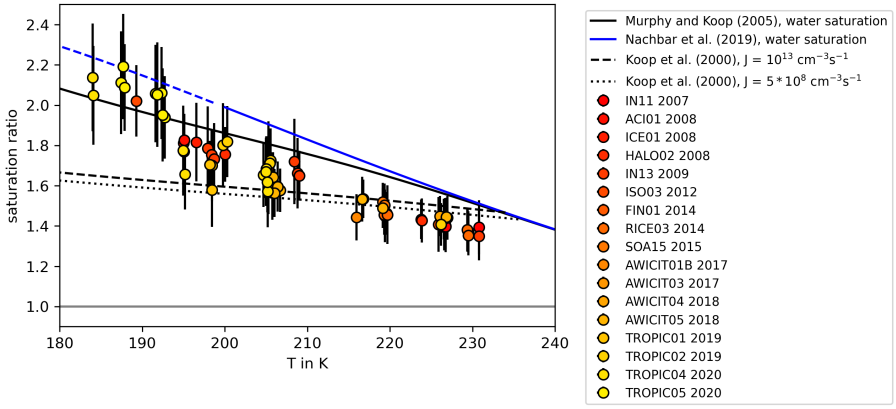

Figure 4. Homogeneous freezing onsets of H_2SO_4/H_2O aerosol particles. The freezing onset conditions, T_{ice} and $S_{ice,fr}$, are displayed in comparison with the homogeneous freezing thresholds suggested by the WAC-based predictions by Koop et al. (2000) (dashed and dotted black lines) and the water saturation pressure with respect to supercooled liquid water according to Murphy and Koop (2005) (solid black line) and according to Nachbar et al. (2019) (solid blue line). The colors represent the different AIDA campaigns in the corresponding years. The oldest campaigns are presented in reddish, whereas the more recent campaigns are shown in yellowish colors.

https://doi.org/10.5194/acp-2021-319
Preprint. Discussion started: 21 April 2021

Atmospheric Chemistry and Physics Discussions

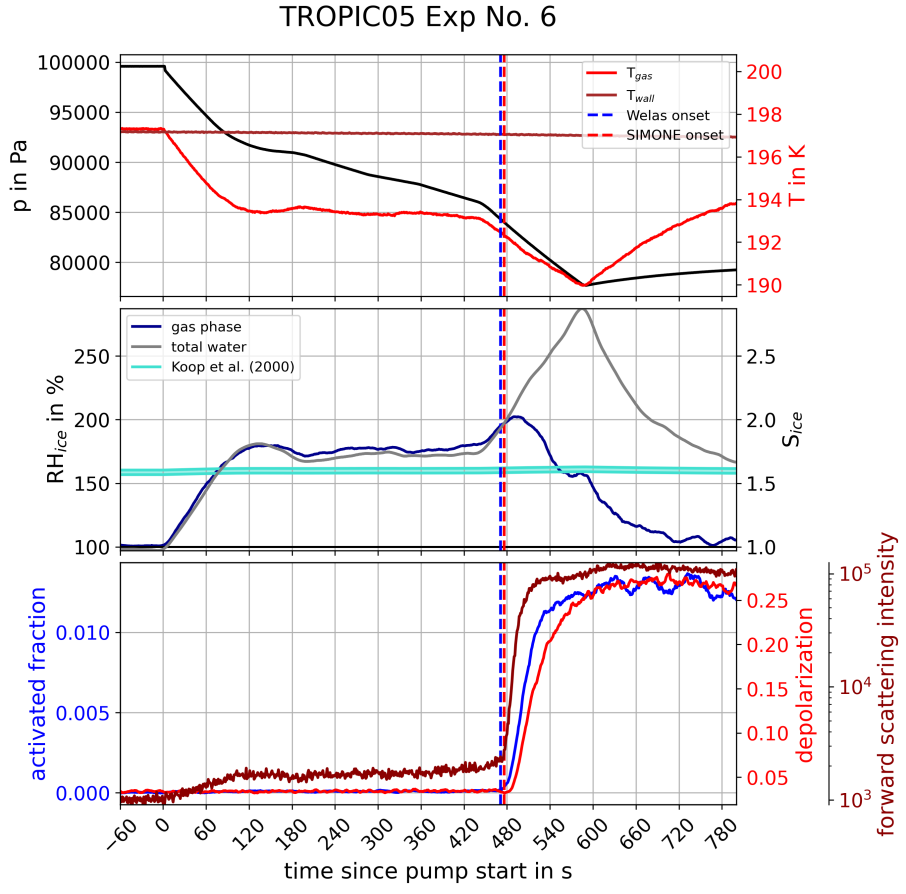

Figure 5. Investigation of kinetic limitations with respect to water uptake in the AIDA chamber. The figure is composed in the same way as Fig. 3. For the experiment shown, started at about 197 K, the pump rate was controlled in such a way that the relative humidity with respect to ice stayed relatively constant for about 5 minutes at about 170 %, hence above the homogeneous freezing threshold suggested by Koop et al. (2000). For details on this experiment see Sect. 3.

https://doi.org/10.5194/acp-2021-319
Preprint. Discussion started: 21 April 2021

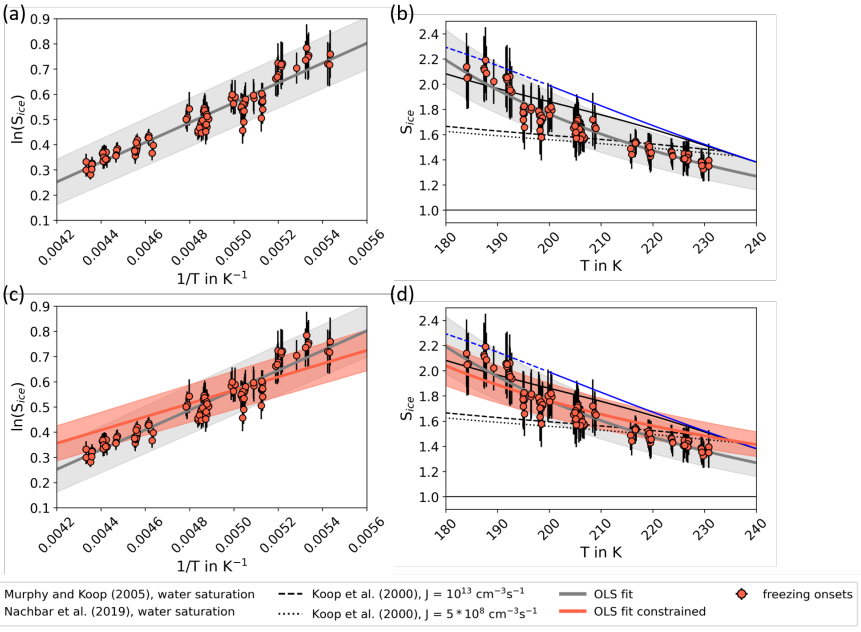

Figure 6. New fit line for homogeneous freezing onsets of H_2SO_4/H_2O aerosol particles. Panel (a): The freezing onsets determined by OPC and SIMONE data (red dots) are shown in an Arrhenius plot and fitted by an ordinary least square (OLS) fit with the form $\ln(S_{ice}) = a + \frac{1}{T} \cdot b$. The parameters are $a = -1.4 \pm 0.05$ and $b = 390 \pm 10\,\mathrm{K}$ and the goodness of the fit is $R^2 = 0.92$. The shaded area is indicative for the uncertainty of the fit parameters. Panel (b): The OLS fit shown in panel (a) is transferred into the S_{ice}-T-space and compared to Koop2000 and the water saturation lines suggested by Murphy and Koop (2005) and Nachbar et al. (2019). Panel (c) and (d): The fit shown in panel a is constrained to the well-known homogeneous freezing conditions of pure water at $T = 235\,\mathrm{K}$ and $S_{ice} = 1.44765$ according to the parameterizations of Murphy and Koop (2005). The fit parameters for the constrained fit (red line) are $a = -0.75 \pm 0.04$ and $b = 263 \pm 8\,\mathrm{K}$ and the goodness of the fit is $R^2 = 0.92$.

https://doi.org/10.5194/acp-2021-319
Preprint. Discussion started: 21 April 2021

Atmospheric Chemistry and Physics Discussions

Table 1. Previous measurements of homogeneous freezing of H_2SO_4/H_2O solutions. The columns show the name of the publication, the used measurement device, the sample volume V, the cooling rate cr (if available) and information about which parameters, weight percentage composition $wt\%$ or the relative humidity RH, were measured or derived to characterize the freezing onsets ('measured' = parameter was directly measured, 'given' = parameter was calculated e.g. using the E-AIM model or others).

	device	V (µl)	cr (K/min)	wt%	RH
Ohtake (1993)	test tube	10000	1	measured	-
Beyer et al. (1994)	capillary	5	2	measured	-
Song et al. (1994)	test tube	2000	-	measured	-
Bertram et al. (1996)	flow tube	$4.2 \cdot 10^{-12}$	-	measured	-
Clapp et al. (1997)	flow cell	$1.4 \cdot 10^{-11}$	-	measured	-
Koop et al. (1998)	cold stage	$6.5 \cdot 10^{-11}$ - $4.2 \cdot 10^{-6}$	10	measured	-
Chen et al. (2000)	CFDC	$6.5 \cdot 10^{-14}$	-	-	measured
Vortisch et al. (2000)	levitated drop	$1.1 \cdot 10^{-4}$	-	measured	-
Prenni et al. (2001)	flow tube	$8.7 \cdot 10^{-11}$	-	given	measured
Cziczo and Abbatt (2001)	flow tube	$2.7 \cdot 10^{-10}$	-	given	measured
Möhler et al. (2003)	AIDA	$6.5 \cdot 10^{-11}$	1 - 0.1	given	measured
Ettner et al. (2004)	levitated drop	0.3 - 5.6	-	given	-
Mangold et al. (2005)	AIDA	$4.2 \cdot 10^{-12}$ - $1.4 \cdot 10^{-11}$	1 - 0.1	-	measured
Beaver et al. (2006)	flow tube	-	-	measured	-
Kanji et al. (2009)	CFDC	$5.2 \cdot 10^{-13}$	-	-	measured
Swanson et al. (2009)	free fall tube	$1.4 \cdot 10^{-8}$	-	-	measured
this study	AIDA	$1.4 \cdot 10^{-14}$ - $7 \cdot 10^{-10}$	0.04 - 4.8	given	measured

Appendix A: Comparison of OPC and SIMONE derived freezing onsets

https://doi.org/10.5194/acp-2021-319
Preprint. Discussion started: 21 April 2021

Atmospheric Chemistry and Physics Discussions

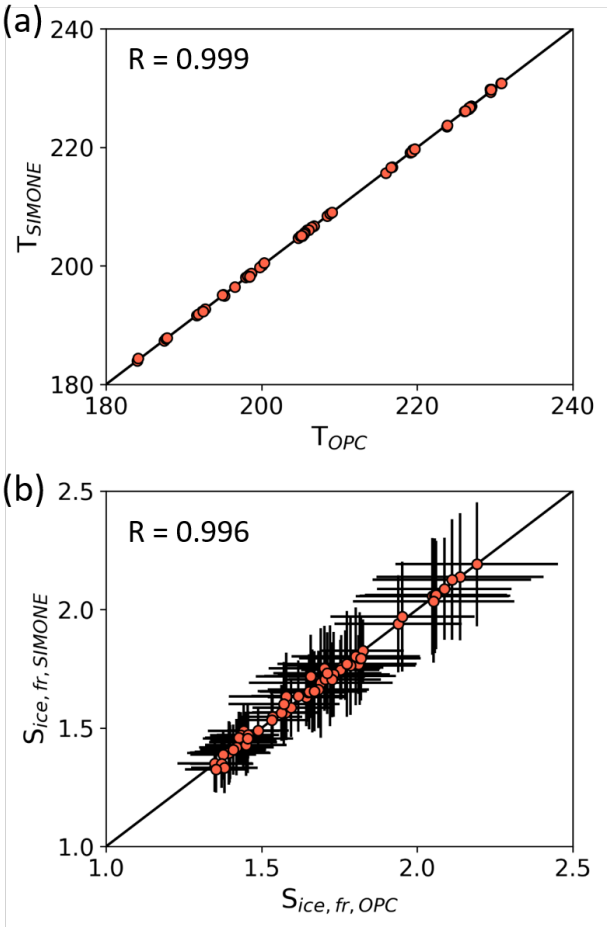

Figure A1. Comparison of the homogeneous freezing onset temperature (T_{ice}, panel a) and ice saturation ratio ($S_{ice,fr}$, panel b) derived from the SIMONE and OPC data. The respective Pearson's correlation coefficients are R = 0.999 and R = 0.996.

https://doi.org/10.5194/acp-2021-319
Preprint. Discussion started: 21 April 2021

Atmospheric Chemistry and Physics Discussions

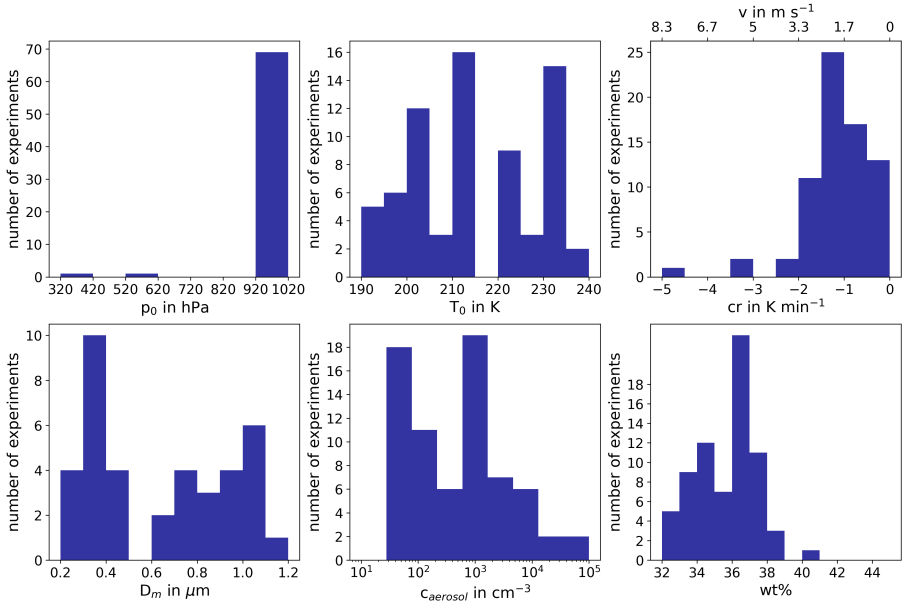

Figure B1. Overview of experimental conditions. The six histograms show the distribution and the parameter range of start pressure p_0, start temperature T_0, cooling rate cr, vertical velocity v, as well as the median aerosol particle diameter D_m, the aerosol particle number concentration $c_{aerosol}$ and weight percentage $wt\%$ of H_2SO_4 in the aqueous solution particles before experiment start.

Appendix B: Overview of AIDA experiments

https://doi.org/10.5194/acp-2021-319
Preprint. Discussion started: 21 April 2021

Atmospheric Chemistry and Physics Discussions

Table B1. Summary of H_2SO_4/H_2O AIDA experiments part I. The considered experiments are listed together with the corresponding campaign, the experiment number, the date of the experiment, the start pressure p_0, the start temperature T_0, the freezing onset temperature T_{ice}, the ice saturation ratio at freezing onset $S_{ice,fr}$, the cooling rate cr and the corresponding vertical velocity v at the freezing onset.

Campaign	Exp No.	date	p_0 (hPa)	T_0 (K)	T_{ice} (K)	$S_{ice,fr}$	cr (K min^{-1})	v (m s^{-1})
ACI01	20	2008-03-06	1016	200	195	1.81 ± 0.07	0.09	0.15
	21	2008-03-06	1016	200	195.1	1.83 ± 0.07	0.52	0.87
	22	2008-03-06	1015	200	195	1.77 ± 0.08	0.23	0.39
	24	2008-03-07	1000	225	219.6	1.46± 0.07	0.47	0.78
AWICIT01B	42	2017-04-12	1005	220	215.9	1.44 ± 0.08	1.15	1.92
AWICIT03	15	2017-09-15	1000	211	205.7	1.60 ± 0.11	0.92	1.54
AWICIT04	6	2018-01-15	994	231	226.6	1.44 ± 0.07	1.23	2.05
	7	2018-01-16	987	231	226.5	1.43 ± 0.07	1.52	2.54
	11	2018-01-17	995	221	216.8	1.54 ± 0.06	0.76	1.27
	37	2018-03-29	996	230	226.1	1.45 ± 0.07	1.2	2.01
AWICIT05	2	2018-06-04	996	231	227	1.44 ± 0.08	1.32	2.2
	4	2018-06-05	997	221	216.6	1.53 ± 0.07	1.1	1.83
	7	2018-06-06	1000	211	205.8	1.64 ± 0.07	0.58	0.96
	8	2018-06-06	999	211	206.7	1.58 ± 0.07	0.81	1.34
	10	2018-06-07	1003	211	206.4	1.60 ± 0.08	0.75	1.24
	15	2018-06-08	998	224	219.1	1.49 ± 0.07	0.88	1.47
	16	2018-06-11	997	231	226.8	1.44 ± 0.07	1.28	2.13
	32	2018-06-18	1012	211	206	1.56 ± 0.08	1.02	1.7
FIN01	25	2014-11-13	999	230	225.9	1.41 ± 0.1	1.48	2.46
HALO02	10	2008-12-11	995	228	223.8	1.43 ± 0.07	0.97	1.62
	11	2008-12-11	998	228	223.8	1.43 ± 0.08	1.88	3.13
	15	2008-12-12	1010	205	200.1	1.76 ± 0.08	1.13	1.88
ICE01	14	2008-06-27	1007	201	196.5	1.82 ± 0.11	1.01	1.69

https://doi.org/10.5194/acp-2021-319
Preprint. Discussion started: 21 April 2021

Atmospheric Chemistry and Physics Discussions

Table B2. Summary of H_2SO_4/H_2O AIDA experiments part II. The considered experiments are listed together with the corresponding campaign, the experiment number, the date of the experiment, the start pressure p_0, the start temperature T_0, the freezing onset temperature T_{ice}, the ice saturation ratio at freezing onset $S_{ice,fr}$, the cooling rate cr and the corresponding vertical velocity v at the freezing onset.

Campaign	Exp No.	date	p_0 (hPa)	T_0 (K)	T_{ice} (K)	$S_{ice,fr}$	cr (K min^{-1})	v (m s^{-1})
IN11	8	2007-11-15	1008	231	226.6	1.40 ± 0.08	1.13	1.89
	9	2007-11-15	1008	231	226.7	1.40 ± 0.08	1.61	2.68
	10	2007-11-15	1008	231	226.7	1.42 ± 0.08	0.5	0.83
	11	2007-11-15	1009	231	226.7	1.40 ± 0.09	0.35	0.58
	46	2007-12-05	1005	236	230.8	1.39 ± 0.1	1.01	1.69
	51	2007-12-07	988	211	205.3	1.69 ± 0.14	0.25	0.42
IN13	30	2009-03-31	585	235	230.8	1.35 ± 0.09	1.16	1.93
	36	2009-04-02	1003	214	208.4	1.72 ± 0.12	0.31	0.52
	37	2009-04-02	1001	214	208.8	1.66 ± 0.11	0.31	0.52
	38	2009-04-02	1001	214	209	1.65 ± 0.07	0.75	1.24
	39	2009-04-03	1005	204	197.9	1.79 ± 0.12	0.59	0.99
	40	2009-04-03	1005	204	198.4	1.75 ± 0.07	0.1	0.16
	41	2009-04-03	1005	204	198.7	1.73 ± 0.1	0.29	0.48
ISO03	43	2012-10-25	320	195	189.3	2.02 ± 0.09	1.3	2.16
RICE03	29	2014-12-11	1003	233	229.4	1.38 ± 0.08	1.34	2.23
	30	2014-12-11	998	233	229.5	1.37 ± 0.07	1.45	2.41
	31	2014-12-11	990	233	229.4	1.38 ± 0.08	1.31	2.19
	32	2014-12-11	1000	233	229.5	1.35 ± 0.07	1.51	2.52
	36	2014-12-15	996	223	219.4	1.45 ± 0.09	1.69	2.82
	37	2014-12-15	1003	224	219.3	1.46 ± 0.07	1.8	3
	38	2014-12-15	1003	224	219.7	1.46 ± 0.1	1.95	3.25
SOA15	77	2015-11-26	1001	223	219.1	1.52 ± 0.06	1.01	1.69
	78	2015-11-26	1003	223	219.4	1.50 ± 0.07	1.31	2.18
TROPIC01	27	2019-07-03	1006	203	198.4	1.70 ± 0.11	2.35	3.91
	28	2019-07-03	1006	203	198.2	1.70 ± 0.07	0.04	0.07
	29	2019-07-03	1006	203	198.5	1.58 ± 0.12	4.84	8.07

https://doi.org/10.5194/acp-2021-319
Preprint. Discussion started: 21 April 2021

Atmospheric Chemistry and Physics Discussions

Table B3. Summary of H_2SO_4/H_2O AIDA experiments part III. The considered experiments are listed together with the corresponding campaign, the experiment number, the date of the experiment, the start pressure p_0, the start temperature T_0, the freezing onset temperature T_{ice}, the ice saturation ratio at freezing onset $S_{ice,fr}$, the cooling rate cr and the corresponding vertical velocity v at the freezing onset.

Campaign	Exp No.	date	p_0 (hPa)	T_0 (K)	T_{ice} (K)	$S_{ice,fr}$	cr (K min^{-1})	v (m s^{-1})
TROPIC02	4	2019-07-09	1004	230	226.2	1.41 ± 0.08	1.08	1.8
	14	2019-07-11	998	211	205.5	1.73 ± 0.09	1.07	1.78
	24	2019-07-16	1002	210	205.4	1.71 ± 0.1	0.97	1.61
	26	2019-07-17	999	205	199.8	1.80 ± 0.11	0.88	1.47
	27	2019-07-17	999	206	200.3	1.82 ± 0.1	1.62	2.7
TROPIC04	2	2020-03-16	1004	210	204.7	1.65 ± 0.1	3.15	5.25
	3	2020-03-16	1004	210	205	1.68 ± 0.1	0.1	0.17
	4	2020-03-16	1004	210	205	1.67 ± 0.1	0.32	0.54
	5	2020-03-17	1014	210	205.2	1.57 ± 0.11	3.19	5.32
	6	2020-03-17	1014	210	205.1	1.62 ± 0.09	0.54	0.9
	15	2020-03-19	1006	200	195.2	1.66 ± 0.11	2.29	3.82
	16	2020-03-19	1006	200	195	1.77 ± 0.13	0.64	1.06
	26	2020-03-24	1015	190	184	2.14 ± 0.13	1	1.67
	28	2020-03-24	1012	190	184.1	2.05 ± 0.12	1.68	2.8
TROPIC05	2	2020-10-12	1005	197	191.6	2.06 ± 0.12	1.05	1.76
	3	2020-10-12	1003	197	192.3	2.06 ± 0.11	1.88	3.14
	4	2020-10-13	999	197	191.8	2.05 ± 0.13	0.54	0.9
	5	2020-10-13	996	197	192.7	1.94 ± 0.11	0.98	1.63
	6	2020-10-13	996	197	192.5	1.95 ± 0.12	1.25	2.08
	7	2020-10-14	999	193	187.4	2.11 ± 0.12	1.27	2.11
	8	2020-10-14	998	193	187.7	2.19 ± 0.12	1.53	2.56
	10	2020-10-15	999	193	187.8	2.09 ± 0.1	0.63	1.05